Hydrogen dispersion in a closed environment

M. de Stefano, X. Rocourt, I. Sochet, N. Daudey

HYDROGEN DISPERSION IN A CLOSED ENVIRONMENT

M. DE STEFANO [a,b], X. ROCOURT[b] , I. SOCHET[b], N. DAUDEY[a]

[a] EDF DIPNN - Direction Technique – 69007 Lyon, France

[b] INSA-CVL, Univ. Orléans, PRISME, EA 4229, F18020, Bourges, France,
xavier.rocourt@insa-cvl.fr

ABSTRACT

The highly combustible nature of hydrogen poses a great hazard, creating a number of problems with its safety and handling. As a part of safety studies related to the use of hydrogen in a confined environment, it is extremely important to have a good knowledge of the dispersion mechanism.
The present work investigates the concentration field and flammability envelope from a small scale leak. The hydrogen is released into a 0.47 m x 0.33 m x 0.20 m enclosure designed as a 1/15 – scale model of a room in a nuclear facility. The performed tests evaluates the influence of the initial conditions at the leakage source on the dispersion and mixing characteristics in a confined environment. The role of the leak location and the presence of obstacles, are also analyzed. Throughout the test, during the release and the subsequent dispersion phase, temporal profiles of hydrogen concentration are measured using thermal conductivity gauges within the enclosure. In addition, the BOS (Background Oriented Schlieren) technique is used to visualise the cloud evolution inside the enclosure. These instruments allow the observation and quantification of the stratification effects.

Keywords: Hydrogen, Dispersion, Small Scale, Leak.

1. INTRODUCTION

The production and consumption of hydrogen in industry is considerable, but its use imposes an accurate analysis of risk characterization to protect the installation and to reduce the potential hazard.
Hydrogen has a low density (about 14 times lower than air at standard temperature and pressure) and a wide range of flammability in air (4% - 75% vol.). These features show that it could disperse quickly during an accidental release and burn easily in the presence of an ignition source. A good understanding of the dispersion and stratification of a hydrogen leak is therefore of fundamental importance in order to better understand the possibility of ignition and explosion of accidental releases.

Over the past decade, many studies have been devoted to understand the dispersion of hydrogen in an enclosed space, experimentally and numerically through CFD codes. In addition, many European research projects, such as HySafe [1], Hyindoor [2] and H2FC [3] were initiated. They aim to support and bring competences and experiences from various research regarding hydrogen safety issues. Within Hyindoor project, safety design guidelines and engineering tool have been developed to prevent and mitigate hazardous consequences of hydrogen release in confined environment [4].
The studies mentioned below were carried out under various conditions such as confined or unconfined, large or small scale, with or without vent. The behaviour of the dispersion of hydrogen depends, in fact, on many factors such as: the discharge conditions (flow, pressure, location and direction), the geometry of the enclosure (size and shape of the enclosure, openings, presence of obstacles), and atmospheric conditions inside and outside the enclosure. Experiments with helium are included as it can be used as a substitute to study the phenomena of hydrogen dispersion for safety reasons. Although the density of helium is twice that of hydrogen, its use is justified at low concentrations [5]. In addition, the tests performed by Swain et al. [6] showed a strong similarity

between helium and hydrogen. They studied the differences between the emissions of two gases using a CFD approach, it is validated by experimental measurements of helium.

Denisenko et al. [7] analysed the mechanisms and kinetics of the evolution of hydrogen clouds in confined spaces of different shapes and sizes and different release conditions. Hydrogen was released in a small scale container of 4 m^3 and in a room with a volume of 25 m^3. Moreover, they have also diffused helium at different velocity in a garage-sized room in order to better understand the role of the flow rate in the distribution of the cloud. The results show that for a given flow rate, it is possible to distinguish two different types of dispersions in a confined enclosure. In their first case, where a low flow rate is maintained, the cloud initially forms in the shape of a layer on the ceiling and then expands downwards. In the second case, where a high flow rate is maintained, the cloud disperses almost uniformly throughout the volume above the discharge point.

Denisenko et al. [7] characterized the difference between the two cases by the value of the Morton number. It is defined as $M = l_s/z$ where l_s is the momentum length scale and z the distance between the point of release and the ceiling. The distance l_s, beyond which the initial specific momentum $M_0 = Q_0 \cdot u_0$ [$m^4 \cdot s^{-2}$] becomes negligible compared to the buoyancy fluxes $F_0 = (Q_0\ g\ \Delta\rho) \cdot (\rho_{air})^{-1}$ [$m^4 \cdot s^{-3}$], it can be estimated from equation (1), as below [8]:

$$l_s = \frac{M_0^{3/4}}{F_0^{1/2}} = \frac{0.96 \cdot u_0 \cdot \sqrt{D}}{\sqrt{\frac{g \cdot (\rho_{air} - \rho_{H_2})}{\rho_{air}}}}\ , \qquad (1)$$

Where u_0 – exit velocity, $m \cdot s^{-1}$; D – diameter of the leak, m; g – acceleration of gravity, $m \cdot s^{-2}$; ρ_{air} – density of air, $kg \cdot m^{-3}$; ρ_{H2} – density of hydrogen, $kg \cdot m^{-3}$.

According to the experimental data, for situations where $M < 1$, there is a stratification of the concentration of hydrogen, whereas for $M >> 1$, a homogenization is observed throughout the room.

Gupta et al. [8] studied the concentration distributions caused by the dispersion of helium in a chamber representing a residential garage (5.76 x 2.96 x 2.42 m^3). The room was equipped with small openings near the base to minimize pressure differences between the interior and exterior of the enclosure, while limiting the loss of the injected gas. They performed four tests based on flow, velocity and injected volume. In all the tests, the cloud formed stratified layers inside the facility. Analysis of the results clearly indicates that the risk of inflammation is highly dependent on the total volume injected rather than the flow rate. Test cases with similar injected gas volumes but different initial conditions (flow rate and injection rate), at the end of the injection phase, show a nearly identical maximum concentration. Subsequent work in the same facility was conducted by Cariteau et al. [9] for studying the effects of exit velocity and vent location on the helium dispersion. The vertical distribution of the volume fraction was analysed for three different ventilation conditions: zero ventilation, open vent at the bottom of the room and open vent at the top of the room. In the third configuration, the exchange rate with the outside was much higher than in the other cases and consequently the presence of an open vent led to reducing the flammable volume. In the case of zero ventilation, the spatial and temporal variations of the volume fraction are in good agreement with the theoretical model of Worster and Huppert [10]. Moreover, Cariteau et al. [9] found that stratification occurs over a wide range of flow rates independently of the opening position. Opening at the ceiling promotes mixing but not enough to produce a homogeneous mixture. Cariteau et al. [11] also studied the dispersion of helium in a small-scale chamber (0.93 x 0.93 x 1.26 m^3). The formation of the stratified layers as a function of the Richardson number (Ri) was examined. The results of these experiments give a clear identification of the three filling regimes: stratified regime, stratified regime with a homogeneous layer and homogeneous regime. For values of the Richardson number greater than unity, it is possible to find a regular stratification similar to that provided by the one-dimensional model of Worster and Huppert [10]. The transition is realized from a number of Ri less than one and the homogeneous regime is verified when the approximate value of Ri is about 0.0032. A CFD benchmark described by Giannissi [12] in which three different vent sizes were examined was performed on the basis of Cariteau et al. experiments [11]. Overall, the simulations exhibited good agreement with the experimental results, especially for the larger vent (900 x 180 mm). The geometric variance (relative scatter) is included in a range that goes from 1 to 1.06. However, in case of smaller vent (900 x 35 mm) the hydrogen concentration in the lower part of the enclosure is over predicted.

Pitts et al. [13] conducted a series of helium dispersion tests in an enclosure measuring 1.5 x 1.5 x 0.75 m^3, which is equivalent to the size of ¼ of a residential garage. They characterized the effects of the location of the gas leak and various sizes and locations of vents on the evolution of concentration profiles during release and post-release periods. Eighteen combinations were studied with two leakage times, three leak positions (centre down, centre up and on the side) and three vent configurations. Comparison of average concentration values for experiments with individual vent in the centre of the front wall, have revealed that the dispersion is not much affected by leak position, release time, and vent size. With two vents, one located near the floor and the other on the ceiling, the average concentration of helium at the end of a discharge is greatly reduced compared to experiments with a single large vent of a similar total ventilation area. These observations indicate that significant amount of air have entered the garage during the release phase. The increase in air infiltration is due to the relatively large pressure difference between the inside and the outside and the lower density of the fluid inside the garage. The use of these data to validate CFD codes has been described in the work of Prasad et al. [14] who used the data from this study to confirm the ability of the CFD code of the NIST FDS to predict helium distributions.
One of the most important studies about the use of data for CFD codes validation was performed by Lacome et al. [15]. It shows the spatial and temporal distribution of hydrogen released inside a cave (7.2 x 3.78 x 2.88 m^3) representing a garage with a single vent near the floor. The study parameters were the flow rate and the duration of injection. The experimental results show that for the cases studied, a clear stratification of a mixture of more or less rich hydrogen can be observed in the upper part of the room. If the duration of injection increases, the layer becomes thicker but its concentration remains relatively homogeneous and constant over time.
One of the tests described by Lacome et al. [15] was the basis for a study led by Venetsanos et al. [16] on the CFD codes capability to predict the distribution of hydrogen. The calculations were performed prior to the availability of the experimental results and then repeated thereafter. In the blind test, there are significant differences between the experimental measurements of hydrogen concentration and the predicted values of the CFD codes. Differences between experimental concentrations and those calculated through codes were reduced after experimental data were available, but discrepancies remain.
Another interesting study for modelling the dispersion of hydrogen with a variety of CFD codes was made by Gallego et al. [17], in collaboration with 12 laboratories by using database of Shebeko et al. [18]. The experiment was carried out inside a cylindrical vessel of 20 m^3. The concentration of hydrogen slowly diffusing through the vessel was measured at 6 points along the axis after the release phase for a period of 250 minutes. These numerical studies have led to the conclusion that CFD models can provide reasonable agreement with the experimental data in case of slow hydrogen dispersion which is supposed to be computationally challenging.
It is important to note that in the most of the studies helium is used for safety reason, the presence of ventilation is studied and the leak is almost always in the bottom part of the enclosure.

This article deals with the analysis of the risks associated with a hydrogen leak in a confined enclosure under non-ventilation conditions and the influence of leak location is studied with different flow rates. In order to facilitate testing and limit the amount of hydrogen, a 1/15 scale enclosure of the represented room of a nuclear facility has been adopted. The simple geometry of the enclosure makes it possible to use the results also in general cases of physical flow behaviour.
The purpose of this study is twofold. First, it consists of experimentally characterizing the hydrogen dispersion according to various parameters such as the flow and the leakage position. Second, it provides a set of reference data to test and validate the ability of CFD codes to predict concentrations and distributions in an enclosure.

2. EXPERIMENTAL SETUP

2.1 Instrumentation

The experimental facility represents a 1/15 - scale model of a room of a nuclear facility. In order to carry out general and non-specific cases, the location taken as a reference is a simple room of a nuclear

facility which contains several obstacles and line portions of the hydrogen, where leakage can occur. The model used is a rectangular enclosure with internal dimensions of 0.47 x 0.33 x 0.20 m^3 length, width and height respectively (Fig. 1).

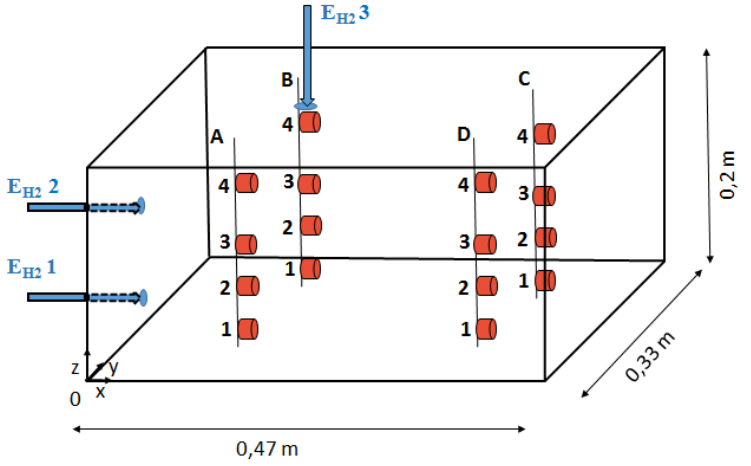

Figure 1. Experimental enclosure scheme and sensor positions.

The enclosure is equipped with a pressure sensor and hydrogen detector placed above the enclosure to control the internal pressure and check for leaks through the box. An air and nitrogen sweep is carried out at the end of the procedure allowing the experimental enclosure to be inerted.

Flow rates at the nozzle exit are measured and controlled with two mass flow controllers (BROOKS). Both controllers can provide accurate flow rates over a range of 0 to 6 $Nm^3 \cdot h^{-1}$, with uncertainties of ± 0.9% on the full scale. The response time of the flux output signals for the flowmeters is less than 2 s.

The hydrogen concentrations are measured using XEN-5320 (Xensor) catharometers. Their small dimensions (sensor diameter d = 0.005 m) and their data rate (3 Hz) make it possible to measure the concentration pointwise every 0.33 s. For an extended concentration measurement, 16 sensors are used inside the installation. They are fixed on four rods, denoted as A, B, C and D in figure 1, with four sensors on each, so as to cover the entire volume. Table 1 summarizes the location of the sensors.

Rod	Position	x (m)	y (m)	z (m)
A	1	0.13	0.07	0.04
	2	0.13	0.07	0.08
	3	0.13	0.07	0.12
	4	0.13	0.07	0.18
B	1	0.13	0.24	0.04
	2	0.13	0.24	0.08
	3	0.13	0.24	0.12
	4	0.13	0.24	0.18
C	1	0.38	0.24	0.04
	2	0.38	0.24	0.08
	3	0.38	0.24	0.12
	4	0.38	0.24	0.18
D	1	0.38	0.07	0.04
	2	0.38	0.07	0.08
	3	0.38	0.07	0.12
	4	0.38	0.07	0.18

Table 1. Positions of the concentration sensors.

The concentration measurements were coupled with visualization. The BOS technique (Background Oriented Schlieren) was used at the jet exit. This method consists of recording a patterned image placed behind the enclosure. In this case the image consists of black square points printed on a white paper sheet. It is first recorded before the beginning of the injection, thus giving an undisturbed reference image. Then, during the release, changes of refractive index in the air / hydrogen mixture are responsible for an apparent deformation of the pattern. The subtraction of the background image from the distorted image allows the optical displacement of the pattern to be seen. The result is a visualization of the density gradient. Dalziel et al. [19] described this method in detail. The images were recorded at the start of the injection with a Phantom VEO 410L high-speed camera with 2000 fps (frame per second) and a resolution of 1024 x 504 pixels.

The enclosure can accommodate pipework obstacles to form congestion (Fig. 2). The reproduction of the obstacles of general room of a nuclear facility is made at 1/15 scale in aluminium. The total volume occupied by the obstacles is 10% of the total volume of the enclosure. They are mobile and can be easily removed. It is manufactured using 3D printer to obtain a design closer to the normal full-scale configuration.

Figure 2. View of the obstacles.

2.2 Test Scenarios

In order to understand the hydrogen dispersion and the behavior of the mixture inside the enclosure, nine test cases are studied with three flow rates for three leakage positions (Fig. 1). All the tests cases have been carried out in a confined enclosure without any ventilation, at ambient conditions of temperature and pressure, in two different configurations with and without obstacles. The outlet diameter d= 0.004 m and the volume injected V= 1.67 L, 5.5% of the enclosure volume, are the defined parameters for all tests. For the laminar case, in the table 2 it can be noted that the total volume of the release is V= 1.47 L, actually the volume injected is V=1.67 L, like the others test cases. The relative gap is due to the regulation of mass control which is slow in case of small flow rate and therefore it injects more than 0.1 $Nm^3 \cdot h^{-1}$ at the beginning of the release. The concentration of hydrogen is measured during the injection phase and after the release for a period of 180 seconds. The increase in pressure inside the enclosure is 74 mbarg and which is quite negligible when considered in the calculation of physical proprieties of hydrogen and air such as density. The three flow rates were chosen in order to study several flow regimes according to different Reynolds numbers, defined by the relation:

$$Re = \frac{\rho_{H_2} \cdot u_0 \cdot D}{\mu_{H_2}}, \quad (2)$$

where ρ – density of hydrogen, $kg \cdot m^{-3}$; u_0 – exit velocity, $m \cdot s^{-1}$; D – diameter of the leak, m ; μ – the dynamic viscosity of the fluid, Pa·s.
The tests cover the three types of regimes: laminar flow (Re < 1000), transitional flow (1000 < Re < 4000) and turbulent flow (Re > 4000).
Table 2 summarizes the parameters for the test cases studied. The coordinates are given in relation to an origin located on the ground at the front of the enclosure on the left edge (Fig. 1).

Reference Flow	Q_1 – Turbulent Flow			Q_2 – Transitional Flow			Q_3 – Laminar Flow		
Reference Position	E_{H2} 1	E_{H2} 2	E_{H2} 3	E_{H2} 1	E_{H2} 2	E_{H2} 3	E_{H2} 1	E_{H2} 2	E_{H2} 3
x release [m]	0	0	0.17	0	0	0.17	0	0	0.17
y release [m]	0.165	0.165	0.165	0.165	0.165	0.165	0.165	0.165	0.165
z release [m]	0.01	0.13	0.2	0.01	0.13	0.2	0.01	0.13	0.2
Release direction	x	x	-z	x	x	-z	x	x	-z
Volumetric flow rate [$Nm^3 \cdot h^{-1}$]		6			1.5			0.1	
Release duration [s]		1			4			53	
Re		4975			1245			85	
Ri		$1 \cdot 10^{-6}$			$1.66 \cdot 10^{-6}$			$3.74 \cdot 10^{-3}$	
l_s [m]		2.66			0.67			0.04	

Table 2. Tests cases for hydrogen releases.

A flow with an inertial force that initially behaves like a jet near the nozzle outlet, can behave like a pure plume in the far field.
The distance l_s, defined by equation (1), is 2.66 m and 0.67 m for the Q_1 and Q_2 tests, respectively. It is greater than the largest dimension of the enclosure which is equal to 0.47 m. For these two test cases the flow structure is of the jet type in the enclosure for both the vertical leak and the horizontal leak. Differently, in the case of Q_3, the distance l_s is equal to 0.04 m, so the flow similar to a plume develops near the exit regardless of the direction of release (vertical or horizontal).
Each case is repeated 5 times to test the consistency of the results. The tests are compared with each other through a detailed analysis. For each sensor, the maximum concentration, ten different concentrations (t = 1 s, 2 s, 3 s, 4 s, 5 s, 10 s, 20 s, 40 s, 50 s, 80 s) and the slopes, in two different time intervals Δt_1 = (40 s - 20 s) and Δt_2 = (90 s - 60 s), of the concentration curves are compared. The results of the comparison shows that the mean relative standard deviation for the ten concentrations is less than 10% for all tests with a minimum of 7%. For the maximum concentration, the average relative standard deviation is 12% for the entry from the ceiling with flow rate Q_2 and 0.6% for the low side leak with Q_3 flow. The comparison of the slopes on the time intervals Δt_1 and Δt_2 shows an average relative standard deviation included between 1% and 18% where the highest differences are visible for the flow rate Q_1, whereas, there are lower differences in respect to the flowrate Q_3. This difference is explained by the fact that the turbulence is heavily present in the case of the flow rate Q_1 and prevents having optimum consistency. In conclusion, the tests are comparable to each other and it is possible to average the 5 tests in order to analyse the results.

3. EXPERIMENTAL RESULTS AND DISCUSSION

3.1 Dependence of leakage flow

In this section, the influence of the flow on the concentration of hydrogen was studied for the case of leakage from the top of the enclosure (E_{H2}-3). The three flows tested represent the three types of flow regimes: the turbulent flow for Q_1, the transitional flow for Q_2 and Q_3 for the laminar flow. The concentration profile of hydrogen in the enclosure with respect to time during the release and the post-release, and an image of the leak at t = 1 s, are shown in figure 3 for the three test cases.

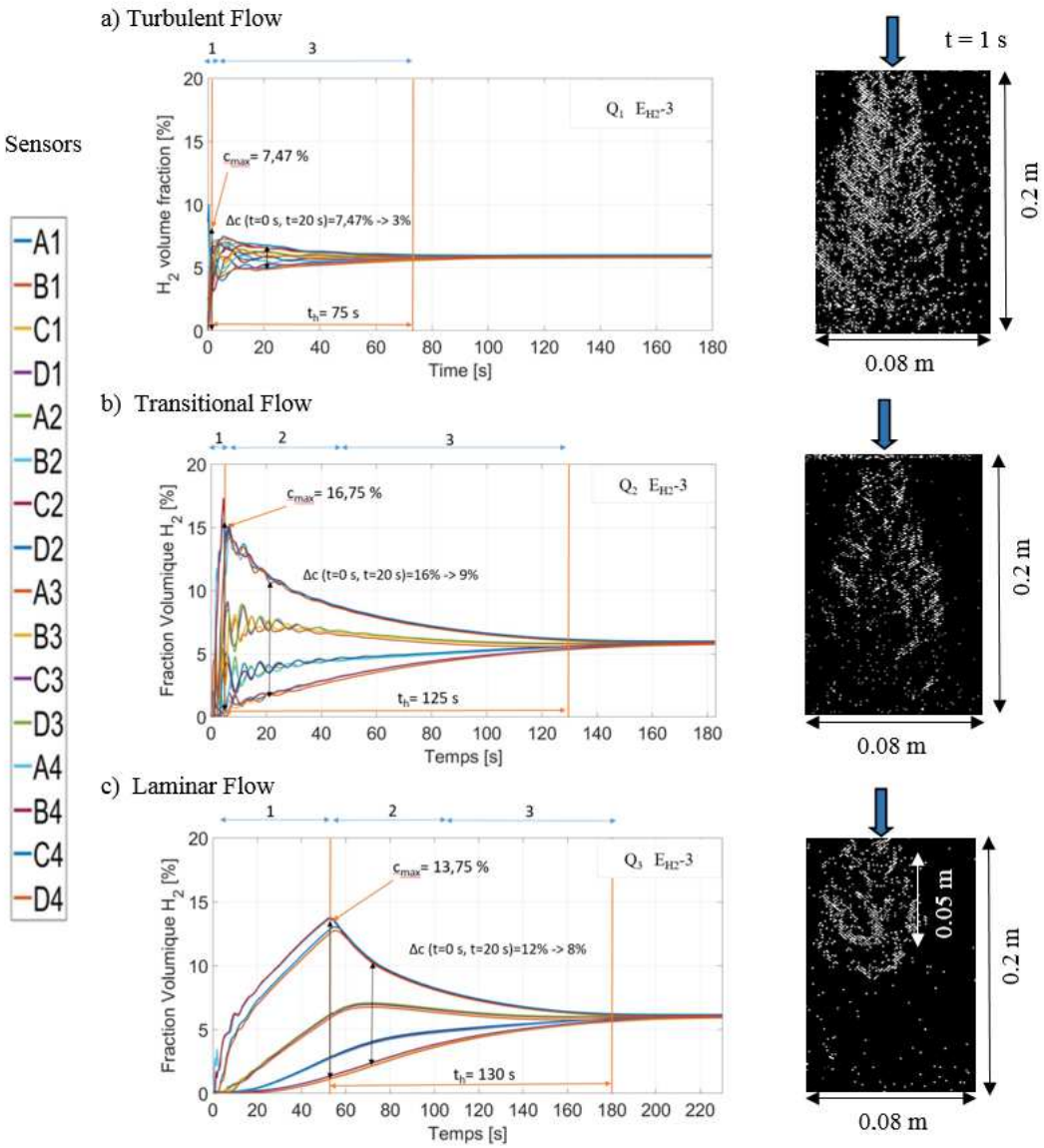

Figure 3. Volume fraction of hydrogen in function of time during the injection and dispersion phases for the 16 sensors, and images obtained at t = 1 s - Leakage from the top - flow rates: a) Q_1 = 6 $Nm^3 \cdot h^{-1}$, b) Q_2 = 1.5 $Nm^3 \cdot h^{-1}$ and c) Q_3 = 0.1 $Nm^3 \cdot h^{-1}$.

By analysing the hydrogen concentration profile as a function of time for all the tests, it is possible to divide the dispersion into three phases: injection, stratification and homogenisation. In the initial phase (injection), the concentration of hydrogen increases immediately, which may be the result of the presence of inertial forces. Peak levels of concentration of hydrogen are detected by the sensors near the ceiling due to buoyancy. The intermediate phase (stratification) following the end of the gas injection, shows that the highest concentrations layers are formed near the ceiling. In this phase, forces induced by inertia begin to decrease and buoyancy begins to dominate the flux. It is also possible to observe well-defined horizontal layers with vertical hydrogen fraction gradient in the enclosure. Once the hydrogen injection is stopped, the concentration becomes homogeneous for all tests during the last phase. Although each test has the same injected hydrogen volume, the concentration profiles are different from each other. In the turbulent case, where Q_1= 6 $Nm^3 \cdot h^{-1}$, the release lasts only 1 s and there is not stratification. The homogenisation takes place very quickly. Hydrogen reaches the ground more rapidly thanks to momentum-dominated forces and allows very rapid homogenization at t= 75 s. In the second case, with Q_2= 1.5 $Nm^3 \cdot h^{-1}$, homogenization is slower and is reached at t = 125 s. Due

to the lower kinetic energy, it is possible to distinguish stratification in the enclosure due to buoyancy. In the laminar case, for Q_3= 0.1 $Nm^3 \cdot h^{-1}$, the jet does not reach the ground. The inertial forces are too small as compared to buoyancy that dominates the flow from 0.05 m after the exit, as can be seen in the associated image (Fig. 2c). The homogenization is reached at t = 130 s after the end of the injection phase, and it occurs mainly because of the molecular diffusion. Consequently, a large gradient of concentration appears, and layers are formed as a function of the height, before the homogenization of the mixture with time. The concentration levels in the upper half of the enclosure decrease, while they increase at the same time in the lower half. These results confirm Cariteau et al. finding [11]. Based on Cariteau et al. study [10] if the injected moment is high enough, the entire volume can be mixed resulting in a constant concentration over the space. If not a vertical stratification takes place. In [11] the limit between the two regimes is Ri= 0.0032, below this value homogenous regime is verified. In this case the limit is much lower, about Ri= $1.5 \cdot 10^{-6}$, because for the transition flow the stratification is still verified.

Significant differences between the three cases are evident for the maximum concentration reached and for the concentration gradient (table 3).

	Turbulent flow	Transient flow	Laminar flow
Maximum concentration [% vol. H_2]	7.47 %	16.75 %	13.75 %
Homogenization time [s]	75 s	125 s	130 s
Concentration variation at t = 20 s after the end of the injection Δc [% vol. H_2]	3 %	9 %	8 %

Table 3. Maximum concentration, homogenization time and gradient concentration for the three types of regimes studied.

In the turbulent case (Q_1) the maximum concentration reached is 7.47 % vol. H_2. For the transient flow (Q_2) and for laminar case (Q_3) the maximum concentration is quite similar and twice as big as the turbulent case. The same might be said for the concentration gradient. For the laminar and transient cases, it is quite similar and three times bigger then the concentration gradient in turbulent case.
In all the tests cases, the hydrogen concentration levels exceed the lower limit of flammability, equal to 4% vol., and therefore the risk of explosion is present.
It is important to note that for all tests the variations in the volume fraction of hydrogen are much greater in the vertical plane than in the horizontal plane. The results of the comparisons between the sensors at the same height show that the average of relative standard deviation for concentrations is less than 5% vol. for all tests.

3.2 Dependence of the leakage position associated with different flow rates

In order to analyse the effects of location and flow rate on the hydrogen dispersion, the comparison of the tests is carried out on two characteristics: the maximum concentration and the time to reach the homogeneous concentration after the end of the injection.
Since the sensors placed at the same height z on the different rods have minimal differences in concentration values, the average of the four curves of the hydrogen volume fraction was made to represent the z planes of the sensors. The comparison of the two characteristics is done as a function of z, in order to have only four points for each case studied, which represent the different heights of the sensors. It is important to note that for the calculation of the homogenization time, only the concentrations obtained during the post-release phase were used, whereas the injection phase was taken into account for the calculation of the maximum concentration.
The maximum concentrations as a function of the height z for the nine cases studied (3 flow rates for 3 injection positions) are shown in figure 4. The cases having the same flow rate are represented with the same colour, while the type of line changes for the different input positions.

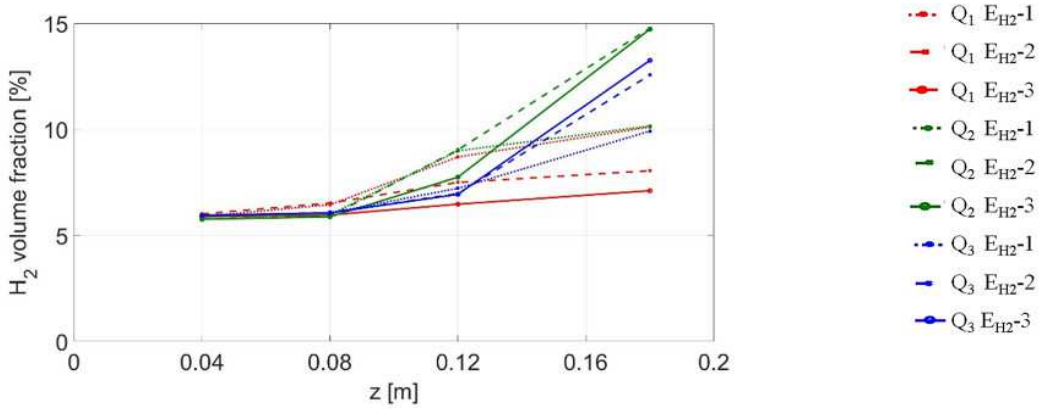

Figure 4. Maximum hydrogen volume fraction versus height z for 3 injection positions (E_{H2}-1, E_{H2}-2, E_{H2}-3) and the 3 flows rates (Q_1, Q_2, Q_3).

From the analysis of figure 4, it is possible to note that the maximum concentration increases with the height for all cases due to the buoyancy of the hydrogen, it results in large accumulation of hydrogen near the ceiling. For the height z = 0.04 m the maximum concentrations are the same for all cases and equal to homogeneous concentration 5.5 %, while for z = 0.18 m the range of values is wider. Increase in height results in more scattered values of hydrogen concentration in all test cases. As regards the influence of the flow rate, as seen above (Fig. 4), the maximum concentration increases with the decrease of the flow rate for the three locations of the leak. It is possible to notice that for z = 0.18 m, the concentration values obtained for the top and top lateral leak locations are similar. The concentration values obtained for the lower side position are distinguished from the others because they are virtually independent of the leakage rate. This is because, for a low flow leak, when the leak is in the lower lateral location, the hydrogen first disperses downwards, while at other locations it immediately rises to the ceiling and reaches the ground only in the last phase (homogenisation phase). In order to confirm this, the maximum concentrations for the lower heights are greater in the case of lower lateral leaks. These results confirm the experiences of Gupta [7] that performed tests with the leak position in the bottom part of the enclosure.

The time, required to reach the homogeneous concentration in the enclosure after the end of the injection for the nine cases studied, is shown in figure 5.

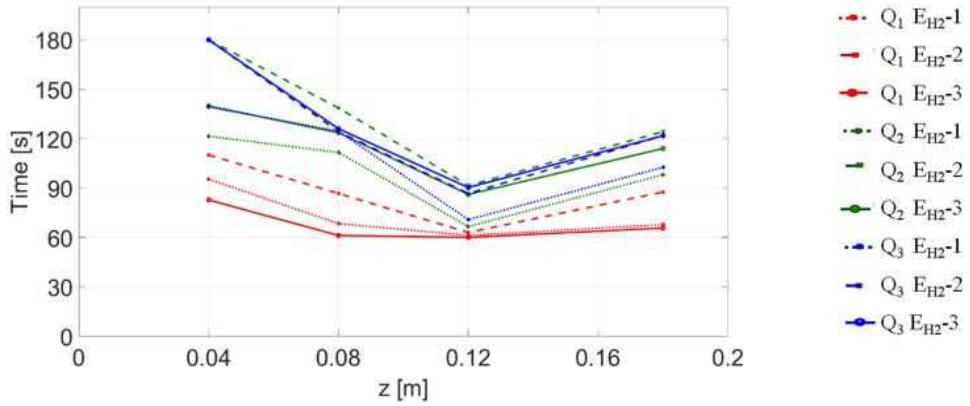

Figure 5. Time to reach the homogeneous concentration inside the enclosure after the end of the injection as a function of the height for the 3 injection positions (E_{H2}-1, E_{H2}-2, E_{H2}-3) and the 3 flows rates (Q_1, Q_2, Q_3).

By comparing the results obtained for the homogenization time after the leak at the different heights, it is noteworthy in all cases that the duration is minimal for z = 0.12 m, while the maximum duration is obtained for z = 0.04 m. This means that for the sensors at the bottom, the homogeneous concentration is reached last regardless of the flow rate and the injection position. On the contrary, for the sensors located at z = 0.12 m, the homogeneous concentration is reached more rapidly. For other heights, the times are similar. As regards the influence of flow, it can be deduced from the graph (Fig. 5) that the homogenization times for all heights and locations increase if the flow rate decreases. This is due to the reduction of the kinetic energy and therefore it results in the reduction of the mixing speed. At low flow rates, in the homogenisation phase, the buoyancy forces dominate the flow relative to the forces induced by the momentum and therefore the phenomenon is slower. When the flow rate increases, it is important to highlight a flattening of the homogenization time curve. This is due to the increase in turbulence and the decrease in the concentration gradient in cases of high flow. The influence of the leakage position is not easy to analyse because if in case of flow rate Q_1 the three curves for different locations are very close, they dissociate in case of flow rates Q_2 and Q_3. Indeed, in the case Q_2 and Q_3 the curves cross each other for the different positions of leak. For the flow Q_1, the smallest homogenization times are achieved with the leak from ceiling, because the distance between the ceiling and the floor is less than the distance between the two side walls and therefore the homogeneous concentration is obtained quickly. For flow rates Q_2 and Q_3, it can be noted that the homogenization time is shorter when the leakage position is on the lower side, while the homogenization time is longer for Q_2 when the leakage is positioned on the upper side.

3.3 Dependency of Obstacles

In order to analyse the hydrogen dispersion in the presence of obstacles, the turbulent flow and laminar flow tests case were performed with obstacles for the case of leakage from the top of the enclosure (E_{H2} 3). This means that the jet impacts the obstacle above 0.02 m. The figure below (Fig. 6) shows the comparison between the hydrogen concentration curves versus time in the case of an empty space and the same in the presence of obstacles, for flow rate Q_1 = 6 $Nm^3 \cdot h^{-1}$ and Q_3 = 0.1 $Nm^3 \cdot h^{-1}$.

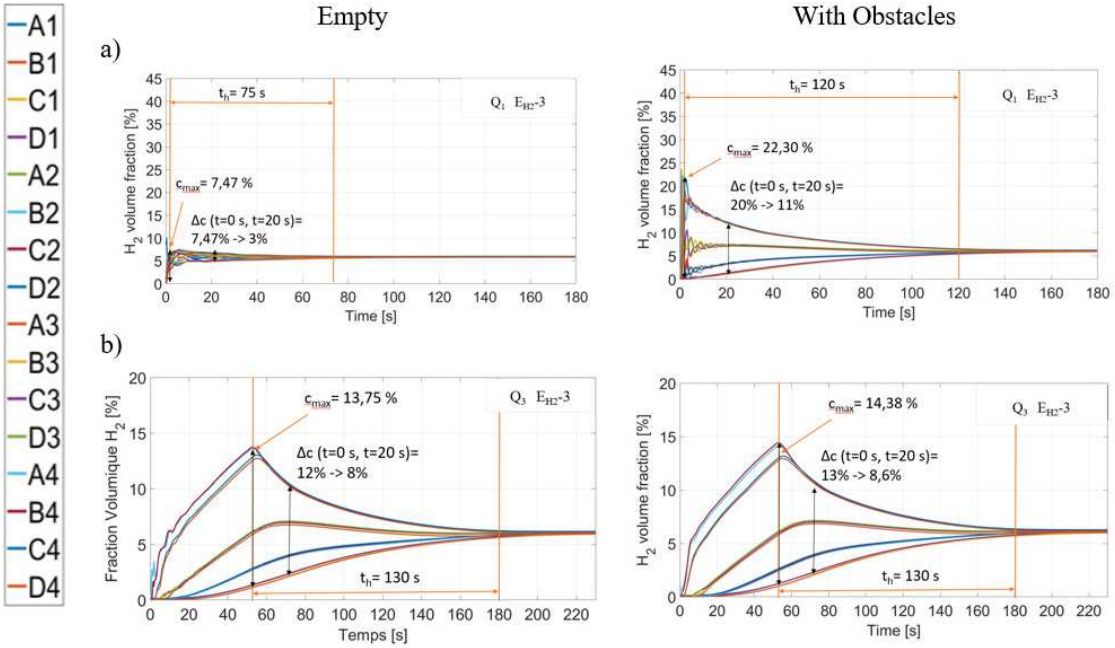

Figure 6. Volume fraction of hydrogen in function of time during the injection and dispersion phases for the 16 sensors - Leakage from E_{H2}-3 - Flow rates: a) Q_1 = 6 $Nm^3 \cdot h^{-1}$, b) Q_3 = 0.1 $Nm^3 \cdot h^{-1}$ without and with obstacles.

The data obtained clearly show that the presence of obstacles influences the dispersion in case of turbulent flow. If the flow is laminar, the dispersion does not change and the hydrogen cloud formed at the end of the leak is the same as in the empty room. For the turbulent flow, the concentration as a function of time changes in the presence of obstacles. The ceiling concentrations are higher and the homogenization times longer compared to the empty chamber. This is due to the fact that the presence of obstacles deflects the injected hydrogen into horizontal direction and causes the loss of the kinetic energy. Table 4 summarizes the main characteristics for the test cases studied.

	Turbulent flow		Laminar flow	
	Empty	With Obstacles	Empty	With Obstacles
Maximum concentration [% vol. H_2]	7.47 %	22.3 %	13.75 %	14.38 %
Homogenization time [s]	75 s	120 s	130 s	130 s
Gradient concentration at t = 20 s after the end of the injection Δc [% vol. H_2]	3 %	11 %	8 %	8.6 %

Table 4. Maximum concentration, homogenization time and gradient concentration for turbulent flow and laminar flow with and without obstacles.

It is important to note that in the case of the jet impacting the obstacles, the concentration gradients are higher. The concentration gradient, in case of turbulent flow increases by three times in presence of obstacles. As a consequence, the time required to homogenization is greater in the case of the room with obstacles (t = 120 s) than in the case of the empty space (t = 75 s).
The risk of explosion will therefore be potentially greater in the presence of obstacles due to the strong impact that they have on the dispersion. Their presence cannot be overlooked.

4. CONCLUSION

In this article, the influence of the hydrogen dispersion in relation to the leak flow rate and location of the leak is analysed in a small-scale confined enclosure with and without obstacles. The volume fraction is measured at ambient temperature and pressure during the release and post-release phase by use of concentration sensors and video capture by the BOS method. Nine combinations of flow and leak position were studied to provide useful information to understand how hydrogen disperses.
For a given leak position, results about the influence of flow rates are in agreement with the results obtained by Cariteau et al. [11] for the similar study. Indeed significant differences for the concentrations is observed between the turbulent flow, Q_1, and the laminar flow, Q_3. By analysing the concentration curves as a function of time, it can be concluded that the higher the flow rate, the faster the hydrogen is dispersed homogeneously in the room. At high flow rate, the kinetic energy dominates the dispersion phenomenon and the hydrogen moves along the periphery of the enclosure until it fills homogeneously. When the flow rate decreases, the dispersion phenomenon is controlled by the buoyancy forces due to the density difference between the hydrogen and the air. Hydrogen, therefore, rises towards the ceiling and forms layers of different concentrations (stratification). The concentration gradients developed during the injection phase dissipate very slowly during the successive phases due to the phenomenon of diffusion. The differences between the two regimes, laminar and turbulent, result in an increase in the maximum concentration, concentration gradients and the time required to homogenise the mixture in the enclosure if the flow rate decreases.
The dispersion depends much more on the flow rate than on the position of the leak. Indeed, the differences between the different positions depend on the flow, the significance of the deviation change in position decreases with the increase in the flow. For a small flow rate it is possible to notice that the hydrogen disperses first at the bottom in the case of lower leakage and it ascends immediately

to the ceiling and only goes down to the homogenisation phase for the other positions. However, it is important to note that for the lower lateral leak for different initial condition the peak concentration levels at the end of injection phase are similar. The obtained results are in a good agreement with the literature study [7].
In the presence of obstacles, the results of the tests make it possible to conclude that if the turbulent jet meets an obstacle, the dispersion mechanism changes. The leak, which in the model with the empty space is controlled by the amount of motion, loses its energy when it impacts the obstacle. Hydrogen, therefore, rises to the ceiling forming higher concentration gradients and therefore has a slower homogenization time.
The experimental results presented in this paper aim to better predict the dispersion of hydrogen in confined spaces. Some of the data presented will be used subsequently to validate the calculations carried out with the FLACS code, in order to predict the scenarios of large scale accidental release of hydrogen.

ACKNOWLEDGEMENTS
The authors acknowledge the support of this research by **EDF DIPNN - Direction Technique**.

REFERENCES

1. HySafe, safety of hydrogen as an energy carrier, project website: http://www.hysafe.org/.
2. HyIndoor. Pre normative research on the indoor use of fuel cells and hydrogen systems. Project website: http://www.hyindoor.eu/.
3. H2FC - Integrating European Infrastructure to support science and development of Hydrogen- and Fuel Cell Technologies towards European Strategy for Sustainable Competitive and Secure Energy, Project website: http://h2fc.eu.
4. Fuster, B., et al., Guidelines and recommendations for indoor use of fuel cells and hydrogen systems, *Int. J. of Hydrogen Energy*, **11**, 2017, pp.7600-7607.
5. Agranat, V., Cheng, Z. and Tchouvelev, A., CFD Modeling of Hydrogen Releases and Dispersion in Hydrogen Energy Station, *Proc. of 15th World Hydrogen Energy Conf.*, 27 June – 2 July 2004, Yokohama, Japan.
6. Swain, M.R., Shriber, J. and Swain, M.N., Comparisons of hydrogen, natural gas, liquified petroleum gas, and gasoline leakage in a residential garage, *Energy & Fuels*, **12**, 1998, pp.83-89.
7. Denisenko, V., Kirillov, I., Korobtsev, S. and Nikolaev, I., Hydrogen-air explosive envelope behaviour in confined space at different leak velocities, *Proc. of 3nd Int. Conf. on Hydrogen Saf.*, 16-18 September 2009, Ajaccio, France.
8. Gupta, S., Brinster, J., Studer, E. and Tkatchenko, I., Hydrogen related risks within a private garage: Concentration measurements in a realistic full-scale experimental facility, *Int. J. of Hydrogen Energy*, **34**, 2009, pp. 5902-5911.
9. Cariteau, B., Brinster, J. and Tkatschenko, I., Experiments on the distribution of concentration due to buoyant gas low flow rate release in an enclosure, *Int. J. of Hydrogen Energy*, **36**, 2011, pp. 2505-2512.
10. Worster, M. and Huppert, H., Time-dependent density profiles in a filling box, *J. of Fluid Mechanics*,**132**, 1983, pp. 457-466.
11. Cariteau, B. and Tkatschenko, I., Experimental study of the concentration build-up regimes in an enclosure without ventilation, *Int. J. of Hydrogen Energy*, **37**, 2012, pp. 17400-17408.
12. Giannissi, S., et al., CFD benchmark on hydrogen release and dispersion in confined, naturally ventilated space with one vent, *Int. J. of Hydrogen Energy*, **40**, 2015, pp. 2415-2429.
13. Pitts, W.M., Yang, J.C. and Fernandez, M.G., Helium dispersion following release in a ¼ scale two car residential garage, *Int. J. of Hydrogen Energy*, **37**, 2012, pp. 5286-5298.
14. Prasad, K., Pitts, W.M. and Yang, J.C., A numerical study of the release and dispersion of a buoyant gas in partially confined spaces, *Int. J. of Hydrogen Energy*, **36**, 2011, pp. 5200-5210.
15. Lacome, J.M., Dagba, Y., Jamois, D., Perrette, L. and Proust, C.H., Large scale hydrogen release in an isothermal confined area, *Proc. of 2nd Int. Conf. on Hydrogen Saf.*, 11-13 September 2007, San Sebastian, Spain.

16. Venetsanos, A.G., et al., An intercomparison exercise on the capabilities of CFD models to predict the short and long term distribution and mixing of hydrogen in a garage, *Int. J. of Hydrogen Energy*, **34**, 2009, pp. 5912-5923.
17. Gallego, E., Migoya, E., Martin-Valdepenas, J.M., Crespo, A., Garcia, J. and Venetsanos, A.G., An intercomparison exercise on the capabilities of CFD models to predict distribution and mixing of H2 in a closed vessel, *Int. J. of Hydrogen Energy*, **32**, 2007, pp. 2235-2245.
18. Shebeko, Y.N., Keller, V.D., Yeremenko, O.Y., Smolin, I.M., Serkin, M.A. and Korolchenko, A.Y., Regularities of formation and combustion of local hydrogen-air mixtures in a large volume, *Chem. & Ind.*, **24**, 1988, pp. 728-731 [in Russian].
19. Dalziel, S.B., Hughes, G.O. and Sutherland, B.R.., Whole-field density measurements by 'synthetic schlieren', *Exp. in Fluids*, **28**, 2000, pp. 322-323.